# GASIFICATION OF THE CHAR DERIVED FROM DISTILLATION OF GRANULATED SCRAP TYRES

Félix A. López[a,1], Teresa A. Centeno[b], Francisco José Alguacil[a], Belén Lobato[b], Aurora López-Delgado[a] and Javier Fermoso[b]

[a] *Centro Nacional de Investigaciones Metalúrgicas CENIM-CSIC, Gregorio del Amo 8, 28040 Madrid, Spain*
[b] *Instituto Nacional del Carbón INCAR-CSIC, Francisco Pintado Fe 26, 33011 Oviedo, Spain*

## Abstract

This work reports the effect of pressure on the steam/oxygen gasification at 1000ºC of the char derived from low temperature-pressure distillation of granulated scrap tyres (GST). The study was based on the analysis of gas production, carbon conversion, cold gas efficiency and the high heating value (HHV) of the product. For comparison, similar analyses were carried out for the gasification of coals with different rank.

In spite of the relatively high ash (≈12 wt%) and sulphur (≈3 wt%) contents, the char produced in GST distillation can be regarded as a reasonable solid fuel with a calorific value of 34 MJ $kg^{-1}$. The combustion properties of the char ($E_A$ ≈50 kJ $mol^{-1}$), its temperature of self-heating (≈264ºC), ignition temperature (≈459ºC) and burn-out temperature (≈676ºC) were found to be similar to those of a semi-anthracite.

It is observed that the yield, $H_2$ and CO contents and HHV of the syngas produced from char gasification increase with pressure. At 0.1 MPa, 4.6 $Nm^3$ $kg_{char}^{-1}$ of syngas was produced, containing 28% v/v of $H_2$ and CO and with a HHV around 3.7 MJ $Nm^{-3}$. At 1.5 MPa, the syngas yield achieved 4.9 $Nm^3$ $kg_{char}^{-1}$ with 30 % v/v of $H_2$-CO and HHV of 4.1 MJ $Nm^{-3}$. Carbon conversion significantly increased from 87% at 0.1 MPa to 98% at 1.5 MPa.

It is shown that the char derived from distillation of granulated scrap tyres can be further gasified to render a gas of considerable heating value, especially when gasification proceeds at high pressure.

**Keywords:** Granulated Scrap Tyres, Distillation, Char, Gasification, Coal.

[1]**CORRESPONDING AUTHOR: FLOPEZ@CENIM.CSIC.ES**

## 1. Introduction

More than 3.4 million tonnes of end-of-life tyres (ELTs) are generated annually in Europe, 234,000 tonnes in Spain (Ramos et al., 2011). European Directive 1999/31/CE bans the disposal of ELTs in landfills, thus European countries have developed different systems for the management of this waste. Spain, for example, runs an integrated management system involving 15 producers/importers and some 36,000 collection points. The system is complemented by classification centres where it is decided which ELTs can be retreaded and which should go into the recovery process to be transformed into a new products or energy.

In the last two years, numerous scrap tyre granulation plants were installed in Europe. The 12 Spanish plants have a treatment capacity of 100,000 tons/year and produce around 65,000 tons/year of steel- and fluff-free granulate textile. This product is classified into three sizes, each with different applications. The fraction below 0.8 mm is used in the manufacture of asphalt, although the market for this product is rather small. The 0.8–2 mm fraction is mainly used in the construction of artificial football turf and other sport-related surfaces, this market suffering from the current lack of public spending. Unfortunately, the 2-12 mm fraction has virtually no market. There is, therefore, an excess production of about 60 tons of this product for which no commercial outlet has been found

Alternatively, this waste can be used in pyrolytic and gasification processes for the production of energy. Pyrolysis is an endothermic degradation process in which a material is heated indirectly in an oxygen-free atmosphere. Tyres pyrolysis results in three main products: pyrolytic oil, gas and char. The yield and composition of each fraction are highly dependent on the experimental conditions such as temperature, heating rate, pressure, residence time, material granulometry and the volatile fraction condensation temperature.

It has been reported that the carbon solid (char) derived from scrap tyre pyrolysis has a small

surface area (around 60 $m^2$ $g^{-1}$) and a high ash (10 wt%) and sulphur (13 wt%) content (Berrueco et al., 2005; Díez et al., 2004; López et al., 2009). However, as a consequence of its calorific value as high as 30 - 40 MJ $kg^{-1}$(Li et al., 2004; Olazar et al., 2008), it may be regarded as a promising solid fuel. Additionally, this carbonaceous material can be upgraded by acid-demineralisation followed by exposure to steam or carbon dioxide to produce activated carbons with similar properties to those commercially available (Ucar et al., 2005; San Miguel et al., 2003).

Gasification is a thermochemical process by which a carbonaceous material (coal, organic wastes, biomass, etc.) can be converted into a gas mainly composed of carbon monoxide and hydrogen, but also with carbon dioxide and light hydrocarbons. The composition markedly depends on the operating conditions such as, temperature and gasifying agent composition (air, oxygen and/or steam), etc. The resulting gas mixture, also called synthesis gas or syngas, can be used as fuel in gas turbines and fuel cells after a cleaning stage, the difficulty and thoroughness of which will depend on the composition of the raw fuel and its final application.

The gasification of waste tyres has been investigated at both laboratory and pilot scales. Galvagno et al. (2009) undertook a comparative study of steam gasification of refuse-derived fuel (RDF), poplar wood, and scrap tyres in a laboratory-scale rotary kiln. The tyres derived-syngas presented high contents of hydrogen (almost 45% v/v), methane, ethylene and ethane, but less significant contribution from oxygenated products. Raman et al. (1981) reported that the gasification of waste tyres in a pilot-scale fluidised-bed reactor produced a syngas with HHV ranging from 22 MJ $Nm^{-3}$ to 39.6 MJ $Nm^{-3}$, as the process temperature decreased from 787ºC to 62ºC. On the other hand, Donatelli et al. (2010) reported the production of high energy syngas by steam gasification of waste tyres in a rotary kiln pilot plant. Their results showed an increasing gas energy content with the steam/tyre ratio to reach a maximum at 0.33. The gas produced under these conditions had a hydrogen content as high as 52.7% v/v and a LHV of,

approximately, 30 MJ $kg_{gas}^{-1}$.

Gasification by air is an exothermic process and results highly promising for the recovery of energy and materials from GSTs (Malkow, 2004; Morris and Waldheim, 1998; Raman et al., 1981; Sharma et al., 1998). Leung and Wang (2003) and Xiao et al., (2008) studied the GSTs gasification with air in a fluidised bed at 350-900ºC. Such a process with an air/GST ratio ranging from 0.2 to 0.6 produced 240-370 kg of char and 0–370 kg of tyre-derived oil (TDO) per tonne of GST. The syngas yield (1.8-3.7 $Nm^{-3}$ $kg^{-1}$) was linearly proportional to the air/GST ratio. The syngas achieved a higher heating value (HHV) of around 6 MJ $Nm^{-3}$. The lower heating value (LHV) increased with increasing temperature or a decreasing air/GST ratio (around 4-9 MJ $Nm^{-3}$).

The development of a combined distillation/gasification unit is novel. Low temperature distillation allows a char of high calorific vlaue to be obtained, which can then be converted into gas. The present paper describes an alternative process for energy recovery from end-of-life tyres, involving the combination of the distillation at low temperature (550ºC) of granulated scrap tyres and the subsequent high temperature gasification of the resulting char.

## 2. Experimental

### *2.1. Materials*

The raw material used in this work was granulated scrap tyres (GST) from the granulating plant GABA (Barcelona, Spain). Basically, it was composed of small particles (<12 mm Ø) of natural and synthetic rubber compounds (63.5%) and carbon black (32.4%) with a little presence of fluff (<2.0 wt%) and steel (<0.1 wt%). Hydrocarbon oils accounts for 2.5%, and the total inorganic compounds (zinc oxide, sulphur and sulphur compounds) achieves 2.5%. Stabilizers and anti-oxidants are also present. Main characteristics are reported in Table 1.

For comparison, four coals of different rank were studied (Fermoso et al., 2010): semi-anthracite (HV), a medium volatile bituminous coal (SA) and two high volatile bituminous coals (PT and DT). For the sake of clarity, their properties are also included In Table 1.

*2.2. Distillation of granulated scrap tyres*

The proposed distillation plant consists of six vertical, tubular, stainless steel reactors (length 1510 mm; wall thickness 6 mm; external diameter 154 mm) operated at batch scale. Each reactor has a capacity of 12 kg GST and is fed through a PN-16 3" type valve. The distillation gas flows out by natural convection and is cooled in two successive condensers (water- and cryogenically-cooled respectively) to recover the oil. The condensers are composed of a number of stainless steel tubes. The upper and lower part of each condenser is equipped with a small expansion chamber for the expansion of gases and the collection of condensed oil. The gas temperature at the entrance of the first condenser is near 250ºC, and at about 100ºC at the exit. The gas reaches the second condenser at 45ºC. Gas condensation is enhanced by a cryogenic cooling system to guarantee a gas temperature below 5ºC in the second condenser. The condensed oils are collected in a deposit equipped with a level-maintaining valve and a pump.

At the bottom of the reactor there is a system to heat the tubes via propane gas. Each tube has three thermocouples, one at the bottom, one in the middle, and one at the top. These, like the rest of the monitoring systems, are connected to a central control unit. When the temperature of the reactor reaches 550ºC, the burners switch off. Whenever the temperature falls they automatically switch on again. The pilot installation has an automated control system that records the temperature measured by the thermocouples. Each batch of GST (12 kg per tube) is heated for 4 h at 550ºC (consumption 0.15 kg propane per kg GST).

The cold gas is cleaned by a three filter system (water, a 1M $Pb(CO_3)_2$ solution, and activated carbon). The clean gas passes through a flowmeter to measure the volume and is conducted to a TOTEM® electric co-generation turbine (Total Energy Module) consisting of a

distillation gas–fed 903 $cm^3$ engine coupled to an engine/alternator. Both are asynchronous. The module has an electronic coupling system that diverts the electricity produced into the Spanish electric grid, and has a system that measures the number of kWh produced.

After completing the distillation process (the endpoint is determined when the rotameter inside the tubing detects total absence of distillation gas), the reactors were cooled for 4 h, opened, and the distillation solids (char) removed by aspiration. The oil was taken from the deposit by using a pump and filtered under pressure. The yields (by weight) of the oil and char fractions were then determined; the difference between the sum of these weights and the weight of the GST equals the weight of the gas. Figure 1 show a flowsheet of the process.

*2.3. Materials characterization*

The proximate and ultimate composition of the materials was determined by using LECO TGA 701 and LECO CHNS 923 analysers. The gross calorific value (GCV) was estimated in an IKAWEEME C4000 automatic bomb calorimeter. Tyre-derived oil (TDO) was also analysed by GC/MS using an AGILENT 7890A gas chromatograph equipped with an AGILENT model MS 5975C mass selective detector and an HP-5MS capillary column (5% diphenyl, 95% dimethyl siloxane).

The flashpoint of TDO was determined using the STANHOPE-SETA Setaflash 3 model, employing the ASTM D1655 method. Since preliminary tests showed the flashpoint to be in the region of 10-20°C, all samples were cooled in a freezer prior to testing.

Kinematic viscosity was determined at 40ºC using a THERMO SCIENTIFIC Haake 1 apparatus.

An automatic distillation test using a PAC Optidis analyser (ASTM D86 method) was performed at atmospheric pressure with a mixture of the distillation oils obtained in several

experiments carried out at 550°C. Experiments were performed between room temperature and the temperature at which no more distilled products could be collected.

The distillation gas (and the gasification gas in the next stage) was collected in Tedlar plastic bags and analysed by gas chromatography using a HEWLETT-PACKARD 5890 gas chromatograph equipped with a thermal conductivity detector, (TCD) and a flame ionisation detector (FID). The carrier gas was He of 99.999% purity and the carrier pressure 0.39 MPa.

The porous characteristics of the char sample were determined using a Beckman Coulter SA1100 automatic adsorption analyser. Total surface area was determined using the BET equation in the $p/p_o$ range 0.015–0.15, ($r^2$>0.9999). The microporosity of the char was analysed using Dubinin's theory. Immersion calorimetry into benzene was performed using a Tian-Calvet type calorimeter (Centeno and Stoeckli, 2010).

The morphological characterization of the char was performed by scanning electron microscopy (SEM) using a field emission Jeol JSM 6500F microscope. For observations, powdered samples were embedded in a polymeric resin. A coating of graphite was used to produce electrically conducting samples.

The crystalline phases in the char were characterized by X-ray diffraction (XRD) using a Bruker XRD Mod. D8 Discover diffractometer ($Cu_{k\alpha}$ radiation, 0.03 2θº step-widths, counting time 5 s per step).

### *2.3. Gasification experiments*

#### *2.3.1. Thermogravimetric analysis*

The distillation char (DC) and coal samples were pulverized to pass through a 100-200 μm mesh (Sang-Woo and Cheol-Hyeon, 2011).

Thermogravimetric analyses (Setaram Sensys Evolution) involved the heating of 30 mg of

the sample at 10ºC $min^{-1}$ up to 1000ºC under 20 ml $min^{-1}$ of pure $O_2$ .

The kinetics of the thermal behaviour of the distillation-derived char (DC) was studied by DTA in non-isothermal conditions at different heating rates between 5 and 20ºC $min^{-1}$. The data recorded (the exothermal peak obtained for the different heating rates) were exported in ASCII format for further thermokinetic interpretation using AKTS-Thermokinetics Software (AKTS, 2010). Kinetic variables were measured using the isoconversional method of Friedman (1964). Friedman analysis, based on the Arrhenius equation, uses the logarithm of the conversion rate *da/dt* as a function of the reciprocal temperature at different degrees of the conversion $\alpha$:

$$\ln \frac{d\alpha}{dT}|\alpha_T = \ln\left(A_i\ f(\alpha_{i,j})\right) - \frac{E_i}{RT_{i,j}} \qquad \text{(Eq.1)}$$

where $E$ is the activation energy (kJ $mol^{-1}$), $A$ is the pre-exponential factor ($s^{-1}$), T is the temperature (K), t is the time (s), R is the gas constant (J $mol^{-1}$ $K^{-1}$), $I$ is the index of conversion, $j$ is the index of the curve, and $f(\alpha_{i,j})$ the function dependent on the reaction model. This is assumed to be constant for a given reaction progress $\alpha_{i,j}$ for all curves $j$.

Since $f(\alpha)$ is constant for each degree of conversion $\alpha_i$, the method is 'isoconversional' and the dependence of the logarithm of the reaction rate on $1/T$ is linear, with a slope of $m = E/R$ and with an intercept of value A.

*2.3.2. Gasification runs*

The gasification of the DC and coals was performed isothermally (1000°C) at pressures of 0.1 and 1.5 MPa, using a mixture of oxygen and steam, 15 and 25 vol%, respectively, as gasifying agent carried on an inert flow of $N_2$. The total gas flow rate was pre-set to each sample composition (carbon content) to ensure constant O/C and $H_2O$/C ratios of 1.3 and 1.1, respectively, at the reactor inlet, maintaining a constant solid flow rate at 5 g $h^{-1}$. The quantities of oxygen and steam introduced with respect to those stoichiometrically necessary, $O/O_e$ and $H_2O/H_2O_e$, were, respectively, 0.4 and 1.5. Figure 2 shows a flow diagram of the experimental device used for the gasification experiments. It consists of a stainless steel tubular downdraft fixed-bed reactor (13 mm internal diameter, 305 mm height) with a porous plate, able to work at a maximum pressure of 2 MPa at 1000°C. Distillation char and selected coals were ground and

sieved to obtain a fraction with a particle size of 75–150 μm. Solid fuel particles were continuously fed into the system from a pressurized hopper, which ensured steady gas production. The mass flow rate of the solids was controlled using a pneumatic actuated valve. The reactor temperature was controlled via a thermocouple connected to a temperature controller and data recorder. This thermocouple was in contact with the sample bed. The pressure was measured by a pressure transducer and automatically controlled by a microvalve (Fermoso et al., 2010). The gas composition of the dried gas fraction ($H_2$, $O_2$, $N_2$, CO, $CH_4$ and $CO_2$) was analysed on-line using a dual channel micro-GC Varian CP-4900 apparatus fitted with a TCD, and equipped with a molecular sieve (Molsieve 5 Å) and a HayeSep A column. Helium was used as the carrier gas.

The system was calibrated using a standard gas mixture at periodic intervals. The amount of gas generated during the experiments was calculated from the nitrogen balance, as the quantity of nitrogen fed into the system was known. The experimental error was determined by calculating the variation in the gas composition in experiments repeated several times on different days. The values obtained were all lower than 4% (Fermoso et al., 2009).

The HHV of the dry gas was calculated as follows:

$$HHV = CO\% \cdot 3018 + H_2\% \cdot 3052 + CH_4\% \cdot 9500 \cdot 0.01 \cdot 4.1868 \quad kJ\ Nm^{-3} \qquad \text{(Eq. 2)}$$

where % denotes the percentage in volume of the dry flue gas components.

Cold gas efficiency, $\eta$ *(%)*, was defined as the ratio between the energy content of the gas and the energy contained in the solid fuel (Lee at al., 1995). It was calculated as follows:

$$\eta = \frac{Y_g \cdot HHV_g}{GCV_c} \cdot 100 \qquad \text{(Eq. 3)}$$

where $Y_g$ is the gas yield calculated as the outgoing dry gas flow rate with respect to the mass flow rate of the dry fuel (char or coal), $HHV_g$ is the gas HHV (kJ $Nm^{-3}$), and $GCV_c$ is the GCV

of the used fuel (kJ $kg^{-1}$).

Finally, the carbon conversion, *X(%)*, was calculated as the total carbon contained in the product gas (C present in CO, $CO_2$ and $CH_4$) with respect to the total carbon contained in the sample fed, according to equation (4):

$$X = Y_g \cdot \frac{CO\% + CO_2\% + CH_4\% \cdot 12}{22.4 \cdot C\%} \cdot 100 \qquad \text{(Eq. 4)}$$

where $Y_g$ is the gas yield and C% is the carbon content of the fuel fed (coal or char).

## 3. Results and discussion

### *3.1. Distillation of the granulated scrap tyres (GST)*

Distillation of the GST at 550ºC generated 46.2±0.3 wt% of oil (TDO), 13.8±0.6 wt% of gas and 39.9±0.8 wt% of char. These oil and char yields were similar to the maximum around 40-58 wt% reported by Cunliffe and Williams (1998) and González et al. (2001) for TDO derived from tyre pyrolysis at 450-550°C. These authors also showed that TDO yield remained essentially constant (40–43 wt%) in the temperature range 500-700ºC. Napoli et al., (1997) and Ucar et al., (2005) illustrated productions of 30-43 wt% of char whereas Mastral et al., (2002) and Berrueco et al., (2005) indicated gas yields ranging from 5 to 55% . These values highly depend on the experimental conditions used for tyre pyrolysis.

Main characteristics of tyres-derived oil are summarized in Table 2. The H/C atomic ratio of around 1.6 indicates that TDO corresponds to a mixture of aromatic and aliphatic compounds, as further corroborated by CG/MS analyses. The carbon and hydrogen contents (85% and 11%, respectively) are comparable to those of refined petroleum fuels and similar tyres-oils obtained by other authors (Laresgoiti et al., 2004; Murugan et al., 2008). Nitrogen percentage is slightly higher than in a light fuel oil but comparable to that of a heavy one. Sulphur content is

significantly lower than the 0.8-1.4 wt% found in similar products (de Marco et al., 2001; Murugan et al., 2009; Ucar et al., 2005) and compares with that of a light-medium fuel oil.

As far as TDO corresponds to an unrefined oil, i.e., a mixture of components with a wide distillation range, its flash point is lower than that of refined petroleum fuels. The LHV reaches 41-43 MJ $kg^{-1}$, in good agreement with those obtained by using other pyrolysis technologies (Olazar et. al., 2008; López et al., 2009).

The density and kinematic viscosity are comparable to that of diesel oil.

An automatic distillation test at atmospheric pressure was performed with a mixture of TDOs obtained in different pyrolysis runs performed at 550ºC. Figure 3 shows that about 24% of the TDO distilled below ≈170°C, which falls within the boiling point range of light naphtha (initial boiling point 160ºC). Around 16% of the components correspond to heavy naphtha, distilling in the range 160-200°C. Finally, ≈ 43% of TDO is a middle distillate (200–350°C). Laresgoiti et al. (2004) report a similar pattern with contributions of 20% naphtha, 10% heavy naphtha and 35% middle distillate, when using a similar technique. Figure 3 also shows that, compared to commercial diesel, the present TDO has a higher proportion of light components (vapour temperature <260°C). This is an advantage since it can be better atomised, with combustion initiating at a lower temperature. However, as a consequence of legal/environmental restrictions, its large amount of heavy products (vapour temperature >287°C) reduces its potential applications.

Table 3 shows that the gas fraction obtained in the GSTs distillation essentially consists of $C_1$-$C_4$ hydrocarbons (mostly methane and n-butane) and $H_2$ with some CO and $CO_2$. The $CO_x$ components may derive from oxygenated organic compounds, such as stearic acid and extender oils, etc., and even from metal oxides or $CaCO_3$, etc.

The $H_2$ content is higher than those reported for tyre pyrolysis-gas by Berrueco et al. (2005).

The volume of gas generated as well as its HHV, largely exceed those quoted in the literature (Galvagno et al., 2002; Laresgoiti et al., 2004; Ucar et. al., 2005; Murugan et. al., 2008). The higher HHV of the present tyre-derived gas derives from the greater proportion of methane and n-butane. The use of this product in a co-generation turbine would produce 440 kWh electricity per tonne of GSTs, the electrical yield of the turbine being around 71% (López et al., 2010).

As summarized in Table 1 the solid carbon residue (char) generated from GST distillation displays interesting characteristics. Its GCV is slightly lower than 30 MJ $kg^{-1}$, suiting values for carbon blacks obtained by other pyrolysis technologies.

The distillation-derived carbon contains a relatively high contribution of ashes (12.5 wt%) as well as 2.8 wt% of sulphur. Inorganic impurities contain Si, Al, Ca, Mg, Na, Ti, Fe and Zn. The content of the latter was similar to that of other chars reported in the literature (Cunliffe and Williams, 1998; Olazar et al., 2008). The XRD spectrum of the char (Fig. 4) reported the presence of zincite (ZnO) and zinc silicate ($Zn_2SiO_4$) in the carbon matrix. Cubic and hexagonal crystals of zincite were confirmed by SEM (Fig. 4-inset). The presence of zincite agrees with previous works. Ucar et al., (2005) and Olazar et al., (2009) illustrated by SEM ZnO and elemental S on the surface of a pyrolytic carbon black obtained at 450-600ºC. Darmstadt et al. (1994) reported that Zn appeared on the carbon black as ZnO at pyrolysis temperatures of below 700ºC, whereas above this temperature it was as α- and β-ZnS (Teng et al., 2000). The presence of zincite is due to the use of zinc oxide as an activator of vulcanisation during tyre manufacture. The appearance of $Zn_2SiO4$ (willenite) is probably due to the reaction between ZnO and the $SiO_2$ also used in tyre manufacture. The mean ZnO content of a tyre is around 2.9 wt% while that of $SiO_2$ is about 5 wt% (Olázar et al., 2009).

The elemental S in the distillation gas was mostly retained in the filter, which contained a $Pb(NO_3)_2$ solution. During the distillation, a very voluminous black precipitate of PbS was produced. However, a high sulphur concentration still remained in the carbon scheleton which

may limit further applications of carbon.

Regarding the textural characteristics of the char, the shape of the $N_2$ adsorption isotherm indicates a main contribution from macropores and wide holes (Fig. 5), with very little adsorption at low pressures but with a rapid increase in adsorption at relative pressures above 0.8. The total pore volume ($p/p_o$=0.98) was approximately 0.4 $cm^3$ $g^{-1}$ and the total surface area of 64 $m^2$ $g^{-1}$. The analysis of the isotherm by the Dubinin-Radushkevich equation provided $E_o$ value below 16 kJ $mol^{-1}$ whereas the enthalpy of immersion of char into benzene, $-\Delta_i H$ ($C_6H_6$), was below 9 J $g^{-1}$. Both parameters confirm the absence of significant microporosity in the solid residue.

*3.2. Gasification of the distillation derived-char*

*3.2.1. Thermogravimetric analysis*

Figure 6a shows the standard combustion stages when the distillation char is subjected to treatment under $O_2$ up to 1000ºC. They consist of: A, the dewatering and oxygen chemisorption period (hasta 191ºC); B, volatilisation and burning (191ºC-338ºC); C, char burning (338ºC – 575ºC); and D, burn-out (575ºC-655ºC). For comparison, TG profiles for coals with different rank, a semi-anthracite (HV), a medium volatile bituminous coal, (SA) and two high volatile bituminous coals (PT, DT), are also included.

Figure 6b illustrates the heat flow associated to the different stages of the process. The first part of the curves corresponds to a global endothermic process, resulting from oxidation reactions (exothermic) and water adsorption (endothermic). This section finishes when oxidation reactions predominate and the global energetic balance begins to be exothermic at the self-heating temperature $T_{sh}$. It is noted that $T_{sh}$ of the various samples clearly differ (Table 4).

After a period of increasing heat loss, a maximum is reached. The burn-out temperature ($T_{ec}$) is obtained when the heat flow is zero. The area under the DTA curve represents the production of

heat during combustion, being related to the GCV value of the sample (Pis et al., 1996). In agreement with the increasing calorific value of the coals, $T_{ec}$ and the DTA curve-area increase markedly with coal rank (Table 4). Regarding the combustion evolution for the char, its $T_{sh}$ is comparable to that of the semi-anthracite, although, in agreement with their volatile matter content, its $T_{ec}$ is slightly higher. As a result, DC shows a slightly longer combustion interval than the coals.

Table 4 also reports the intervals of the combustion temperatures for the coals (191-695ºC) and the distillation char (283-688ºC). The DTA curves of Figure 6b illustrate two clear exothermic peaks for the volatile matter combustion. They are markedly less significant for the semi-anthracite (HV) and the distilled char (DC), due to their much lower volatile content compared to the bituminous coals. In the stage C, the marked exothermic peak for all the samples indicates a high heat release. The ignition temperatures (determined according to Wang et al. (2009)) varied between 355ºC and 460ºC for the coals, strongly depending on the rank. The distilled char and semianthracite presented values around 460ºC.

The TG analysis provides slightly higher ash content than that found by proximate analysis (see Tables 4 and 1, respectively). Such discrepancy may be related to the cylindrical shape of the burning chamber in the TG apparatus, hindering the access of oxygen to the fuel at its bottom. Therefore, combustion would take longer than expected to complete the burnout stage, leaving more ash than estimated by chemical analysis.

### *3.2.2. Kinetics. Influence of the heating rate on the char combustion*

Figure 7 shows the DTA curves for the combustion of the distillation char at different heating rates (5-20ºC $min^{-1}$). The dependence of the logarithm of the reaction rate ($d\alpha/dt$) on *1/T* is linear, with a slope of $m = E/R$ and with an intercept value of A, as shown in Figure 8a. Figure 8b

shows the values of the activation energy ($E$) and the pre-exponential factor ($A$) as functions of the progress of char combustion. $E$ and $A$ were not constant over the course of the reaction. As the reaction progressed ($0< \alpha< 1$), the $E$ of the char ranged from 13 to 479 kJ mol $^{-1}$, and $A$ varied between $1.4 \cdot 10^{7}$ and $8.9 \cdot 10^{31}$ $s^{-1}$. The changes in $E$ suggest that thermal degradation occurs in three stages: volatilisation and burning ($0.1 \leq \alpha \leq 0.30$), char burning ($0.30 \leq \alpha \leq 0.95$) and burnout ($0.95 \leq \alpha \leq 1$). This behaviour agrees with that proposed for a semi-anthracite by Wang et al. (2009). The mean $E$ for the combustion of the char ($0 \leq \alpha \leq 1$) was 46.4 kJ $mol^{-1}$ and the mean $A$ was $3.47E^{2}$ $s^{-1}$ over the temperature range 220-700ºC. The $E$ of the char compares with that of a semi-anthracite (≈50 kJ $mol^{-1}$) (Kök, 2005; Otero et al., 2008).

*3.2.3. Gasification experiments*

Figure 9 illustrates the composition of the gaseous product obtained by the gasification of the distillation char and different coals at 0.1 and 1.5 MPa. In order to evaluate the differences between the experimental data and values derived from the thermodynamic equilibrium, a gasification reaction equilibrium model (Morley, 2005) based on the minimization of the total Gibbs free energy was used. Experimental results have been reported in a previous paper (Fermoso et al., 2010). From the equilibrium values, it can be seen that syngas ($H_2$ + CO) production was favoured at atmospheric pressure whereas the amount of $CO_2$ and $CH_4$ increased with pressure. According to Le Châtelier's Principle, when the pressure of a system is increased there is a shift in the equilibrium of the gas phase reactions to the side which has the smallest number of moles in the gas phase (Eqs. 5 and 6) (Sue-A-Quan et al., 1991; Atimtay et al., 1998).

dry reforming

$$CH_4 + CO_2 \leftrightarrow 2CO + 2H_2 \qquad \text{(Eq. 5)}$$

steam reforming:

$$CH_4 + H_2O \leftrightarrow CO + 3H_2) \qquad \text{(Eq. 6)}$$

The fact that DC at 1.5 MPa produced 2% more syngas than at atmospheric pressure disagrees with the predictions based on thermodynamic equilibrium analysis. However, this difference falls within the experimental error.

In the case of the coals, the effect of reaction pressure on devolatilisation stage during the gasification process has to be considered. Relevant differences may appear in the morphology and reactivity of the devolatilized product, and these affect the heterogeneous reactions and the gas composition. At atmospheric pressure, a higher and faster release of volatile matter occurs, leading to a reduction in the amount of char produced (Saxena, 1990; Griffin et al., 1994). Furthermore, the higher porosity development and the lower ordering degree of carbon will enhance the reactivity. On the other hand, an increase in the pressure system will lead to lower fuel devolatilisation, as the pressure exerted from the inside by the volatile matter is counteracted by the external pressure. The process at 1.5 MPa results in a higher amount of char but it is more ordered and less reactive (Chen et al., 2008; Wu et al., 2000; Miura et al., 1989). The higher reactivity of carbon towards oxygen than to steam would explain the enhancement of $CO_2$ production (eq. 7) at 1.5 MPa. On the contrary, as $H_2$ and CO are mainly generated through steam gasification reaction (eq. 8), their production was hindered at high pressure.

Carbon oxidation: $C + O_2 \rightarrow CO_2$; Eq. (7)

Carbon steam gasification: $C + H_2O \leftrightarrow CO + H_2$ Eq. (8)

The distillation char achieved the maximum generation of oxygenated species (CO and $CO_2$), followed by the semi-anthracite. This is related to the potential to produce these species as the carbon content increases. On the other hand, the lower $H_2$ production with the distillation char compared to coal gasification appears to derive from the high oxygen content employed in the gasifying agent ($O/O_e = 0.4$) and the higher reactivity of DC.

Table 5 summarizes the main characteristics of the gas produced during to the gasification

experiments at pressures of 0.1 and 1.5 MPa. As the total gas flow rate was pre-set to maintain constant the O/C ratio, the higher carbon content of DC and the semi-anthracite enhanced the gas production. As a consequence of the higher total gas flow rate used, the gas generated from the DC and HV was more diluted by the $N_2$ introduced and had a lower HHV. Therefore, the higher production of $H_2$ by the bituminous coals provided higher HHV. Lower rank coals showed greater carbon conversion to gas since they react more strongly with the gasifying agent at atmospheric pressure (see Table 5).

The distillation char was nearly all transformed into gas (X = 97.5%) at 1.5 MPa, while the conversion for the coals did not exceed 92-93%. Higher pressure led to an increase in the HHV (from 3.7 to 4.1 MJ $Nm^{-3}$) and recovery (from 4.6 to 4.9 $Nm^{-3}$ $kg_{char}^{-1}$) of gas. Additionally, the gas is richer in $H_2$ and CO (Table 5). These results are similar to those reported by Xiao et al., (2008) for the direct gasification of scrap tyres using a fluidised bed. In the latter system, gases with LHV of 4-9 kJ $Nm^{-3}$ were obtained and a gas recovery of 1.8-3.7 $Nm^{-3}$ $kg^{-1}$ recorded for gasification temperatures of 600-800ºC. Similar cold gas efficiency, $\eta$ *(%)*, were obtained during the gasification of the char and semi-anthracite. As opposed to coals, $\eta$ for DC increased significantly with the reaction pressure.

The syngas obtained in char gasification, which had an HHV of some 3.7-4.1 MJ $Nm^{-3}$ (depending on the gasification pressure), falls within the low calorific value (LCV) fuel range. This is similar to that obtained in the gasification of plant biomass, and can be used by boilers, burners, internal combustión engines and gas turbines, although the latter would need to be adapted (Adouane et al., 2002; de Jong et al., 2003).

The combined process of GST distillation plus char gasification thus led to the final production of a syngas with a very high HHV ($HHV_{distillation\ gas}$ = 68.7 MJ $Nm^{-3}$ and $HHV_{gasification\ gas} \approx$ 4 MJ $Nm^{-3}$) and a high gas recovery (Gas $recovery_{distillation}$ = 46.5 MJ $kg^{-1}$ and Gas $recovery_{gasification}$ 4.6-4.9 MJ $kg^{-1}$). These values are higher than those achieved by the direct tyres gasification.

The $H_2$ content of the syngas (about 23% v/v) obtained with the present experimental device is lower than in the gases released by direct tyre gasification (45-53% v/v) in a rotatory kiln reactor (Galvagno et al., 2009; Donatelli et al., 2010). On the contrary, the syngas obtained by the present combined process has greater $C_xH_y$ contents. The combined process also produces TDO (around 46.2 kg/100 $kg_{GST}$) and solid wastes (about 6-10 kg/100 $kg_{GST}$) as subproducts of char gasification. The solid residue content was estimated from the char ash and the degree of conversion achieved in the gasification process.

The cold gas efficiency of the present process varies from 74-84%, depending on the gasification pressure. This suggests that the gasification of the char is an essential step for the recovery of energy from GST, independently of the gasification pressure. The ignition temperature, burn-out temperature and activation energy of the distilled char (DC) are all similar to those obtained for semi-anthracite (HV). The combined distillation/gasification process, therefore, would offer an interesting alternative for recovering energy from scrap tyres, especially from their post-distillation char. The physico-chemical characteristics of this char do not compete with commercial carbon blacks subjected to strict standards. The demineralisation and activation of the distillation char to produce an activated of competitive quality would be too costly. The demineralisation of the char in an adicid medium at room temperature allows the Zn in the form of ZnO to be diminished, although it would be difficult to eliminate the Zn associated with $Zn_2SiO_4$. This would require alkaline attack at high pressure – an expensive undertaking.

## 4. Conclusions

The present results show that, at atmospheric pressure, the distillation of granulated scrap tyres at moderate temperature (550ºC) in a low oxygen atmosphere is a viable way of making use of scrap tyres.

The yields of the different fractions obtained are similar to those reported in the literature when using other pyrolysis techniques employing a nitrogen atmosphere. Distillation, however, has the advantage of technological simplicity, lower investment costs, and the minimization of secondary reactions due to short reactor residence times. Consequently, high yields of olefins are obtained in the gaseous stream (33.5 vol% of n-butane at 550ºC). Further, the process obtains high yields of oils (46 wt%). The quality of the residual char is comparable to that of some commercial carbon blacks.

In addition, the distillation char could be gasified obtaining a gas product with considerable heating value, especially when gasification proceeds at higher pressure. But also, this char could be co-gasified at existing coal gasification plants without any modification of the gasifier. Distillation and gasification presents new perspectives for upgrading granulated scrap tyres.

**ACKNOWLEDGEMENTS**

This work was funded by ENRECO 2000 Ltd.

## References


Adouane,B., Hoppesteyn,P., de Jong,W., van der Wel,M., Hein, K.R,G and Spliethoff,H., 2002. Gas turbine combustor for biomass derived LCV gas, a first approach towards fuel-NOx modelling and experimental validation**.** Appl. Therm. Eng. 8, 959-970.

AKTS AG, Advanced Thermokinetics software. Vs. 3.25. Switzerland.

Atimtay,A.T., Harrinson, D.P., 1998. Desulfurization of Hot Coal Gas. Springer, Berlin.

Berrueco, C., Esperanza, E., Mastral, F.J., Ceamanos J. , García-Bacaicoa, P., 2005. Pyrolysis of waste tyres in an atmospheric static-bed batch reactor: Analysis of the gases obtained. J.Anal.Appl.Pyrolysis 74 (1-2), 245-253.

Centeno, T.A., Stoeckli, F., 2010. The assessment of surface areas in porous carbons by two model-independent techniques, the DR equation and DFT. Carbon 48(9), 2478-2486.

Chen,H., Luo,Z., Yang,H., Ju,F., Zhang, S., 2008. Pressurized pyrolysis and gasification of Chinese typical coal samples. Energy Fuels 22, 1136-1141.

Cunliffe M.A., Williams P.T., 1998. Composition of oils derived from the batch pyrolysis of tyres. J.Anal.Appl.Pyrolysis 44, 131–152.

Darmstadt, H., Roy, C. , Kaliaguine, S.,1994. ESCA characterization of commercial carbon blacks and of carbon blacks from vacuum pyrolysis of used tires. Carbon 32(8), 1399-1406.

De Marco Rodriguez, I., Laresgoiti, M. F., Cabrero, M. A., Torres, A., Chomón, M.J. , Caballero, B., 2001. Pyrolysis of scrap tyres. Fuel Process.Technol. 72 (1), 9-22.

De Jong, W.,Ünala,O., Andriesa,J, Heina, K.R.G., and Spliethoffa, H. 2003. Biomass and fossil fuel conversion by pressurised fluidised bed gasification using hot gas ceramic filters as gas cleaning. Biomass Bioenerg. 25, 59-83.

Donatelli, A., Iovane, P., Molino, A.,2010. High energy syngas production by waste tyres steam gasification in a rotary kiln pilot plant. Experimental and numerical investigations. Fuel 89 (10),2721-2728.

Díez, C., Martínez, O., Calvo, L. F., Cara, J., Morán, A., 2004. Pyrolysis of tyres. Influence of the final temperature of the process on emissions and the calorific value of the products recovered. Waste Manage. 24(5), 463-469.

Fermoso, J., Arias, B., Gil, M. , Plaza, M.G., Pevida, C., Pis, J.J., Rubiera, F., 2010. Co-gasification of different rank coals with biomass and petroleum coke in a high-pressure reactor for $H_2$-rich gas production. Biosour.Technol. 101 (9), 3230-3235.

Fermoso, J., Arias, B., Plaza, M.G., Pevida, C., Rubiera, F., Pis, J.J., García-Peña,F., Casero, P., 2009. High-pressure co-gasification of coal with biomass and petroleum coke. Fuel Process. Technol. 90, 926-932.

Friedman, H.L., 1964. Kinetics of thermal degradation of char-forming plastics from thermogravimetry. Application to phenolic plastic. J.Polym.Sci., Part C: Polymer Synposium, 6PC, 183.

Galvagno, S., Casu, S., Casabianca, T., Calabrese, A., Cornacchia, G. 2002. Pyrolysis process for

the treatment of scrap tyres: preliminary experimental results. Waste Manage. 22(8), 917-923.

Galvagno, S., Casciaro, G., Casu, S., Martino, M., Mingazzini, C., Russo, A., 2009. Steam gasification of refuse-derived fuel (RDF); influence of process temperature on yield and product composition, Waste Manage. 29, 678–689.

González, F., Encinar, J.M., Canito, J.L.,Rodríguez , J.J., 2001. Pyrolysis of automobile tires wastes. Influence of operating variable and kinetic study. J.Anal.Appl.Pyrolysis 58–59, 667–683

Griffin, T.P., Howard, J.B., Peters, W.A., 1994. Pressure and temperature effect in bituminous coal pyrolysis: experimental observations and a transiet lumped parameter model. Fuel 73, 591-601.

Kök. M.V., 2005. Temperature-controlled combustion and kinetics of different rank coal samples. J.Therm. Anal.Calorim. 79, 175-180.

Laresgoiti, M.F., Caballero, B.M., de Marco, I., Torres, A., Cabrero M.A., Chomón, M.J., 2004. Characterization of the liquid products obtained in tyre pyrolysis. J.Anal.Appl.Pyrolysis 71, 917–934.

Lee, J.M., Lee, J.S., Kim, J.R., Kim, S.G., 1995. Pyrolysis of waste tires with partial oxidation in a fluidized-bed reactor. Energy 20 (22), 969-976.

Leung, D.Y.C., Wang, C.L., 2003. Fluidized-bed gasification of waste tire powders. Fuel Process. Techonol. 84 (1-3), 175-196.

Li, S.-Q., Yao, Q., Chi, Y., Yan, J.H., Cen, K.F., 2004. Pilot-Scale Pyrolysis of Scrap Tires in a Continuous Rotary Kiln Reactor. Ind. Eng. Chem. Res. 43(17), 5133-5145.

López, G., Olazar, M., Artetxea, M., Amutioa, M., Elordia, G.,Bilbao, J., 2009. Steam activation of pyrolytic tyre char at different temperatures. J.Anal.Appl. Pyrolysis 85(1-2), 539-543.

López, F.A., Centeno, T.A., Alguacil, F.J., Lobato,B., López-Delgado, A., Fermoso, J. 2010. Distillation and gasification of granulated scrap tyres for production of electric power. G10 *In: Proceedings Venice 2010, Third International Symposium on Energy from Biomass and Waste Venice, Italy; 8-11 November 2010. Edited by International Waste Working Group. ISBN:978-88-6265-008-3.*

Malkow,T., 2004. Novel and innovative pyrolysis and gasification technologies for energy efficient and environmentally sound MSW disposal. Waste Manage. 24, 53-79.

Mastral, A.M., Callen, M.S., Murillo, R., García, T., López, I.M., 2002. Polyaromatic hydrocarbons in flue gases from waste tire combustion, Polycyclic Aromat. Compd. 22(3-4), 561-570.

Miura, K., Hashimoto, K., Silveston, P.L., 1989. Factors affecting the reactivity of coal chars during gasification, and indices representing reactivity. Fuel 68, 1461-1475.

Morley, C., 2005. GASEQ: A chemical equilibrium program for Windows. Vs. 0.79.

Morris, M., Waldheim,L., 1998. Energy recovery from solid waste fuels using advanced gasification technology. Waste Manage. 18, 557–564.

Murugan, S., Ramaswamy, M. C., Nagarajan, G., 2008. The use of tyre pyrolysis oil in diesel engines. Waste Manage. 28 (12), 2743-2749.

Murugan. S., Ramaswamy, M.C., Nagarajan, G., 2009. Assessment of pyrolysis oil as an energy

source for diesel engines. Fuel Process.Technol. 90(1), 67-74.

Napoli, A., Soudais,Y., Lecomte, D., Castilllo, S., 1997. Scrap tyre pyrolysis: Are the effluents valuable products?. J.Anal.Appl.Pyrolysis 40–41, 373-382.

Olazar,M., Aguado, R., Arabiourrutia, M., Lopez, G., Barona, A., Bilbao, J., 2008. Catalyst effect on the composition of tire pyrolysis products. Energy Fuels 22, 2909–2916.

Olazar, M., Amutio, M., Aguado, R., Bilbao, J., 2009. Influence of tire formulation on the products of continous pyrolysis in a conical spouted bed reactor. Energy Fuels 23, 5423-5431.

Otero, M., Gómez, X., García, A.I., Morán, A., 2008. Non-isotehermal thermogravimetric analysis of the combustion of two different carbonaceous materials. Coal and sewage sludge. J.Therm.Anal.Calorim.93 (2), 619-626.

Pis, J.J., de la Puente, G., Fuente, E., Morán, A., Rubiera, F., 1996. A study of the self-heating of fresh and oxidized coals by differential thermal analysis. Thermochim.Acta 279, 93-101.

Raman, K.P., Walawender, W.P., Fan, L.T., 1981. Gasification of waste tires in a fluidized reactor. Resource.Conserv.Recycl. 4, 79–88.

Ramos, G., Alguacil, F.J., López, F.A., 2011. The recycling of end-life tyres. Technological Review. Revista de Metalurgia. DOI: 10.3989/revmetalmadrid.1052.

San Miguel G., Fowler G.D., Sollars C.J., 2003. A study of the characteristics of activated carbons produced by steam and carbon dioxide activation of waste tyre rubber. Carbon 41(5), 1009-1016.

Sang-Woo, P. , Cheol-Hyeon, J., 2011. Characteristics of carbonized sludge for co-combustion in pulverized coal. Waste Manage. 31,523-529.

Saxena, S.C., 1990. Devolatilization and combustión characteristics of coal particles. Prog. Energy Conbust. Sci. 16, 55-94.

Sue-A-Quan, T., Watkinson,A.P., Gaikwad,R.P., Lim, C.J., Ferris, B.R., 1991. Steam gasification in a pressurized spouted bed reactor. Fuel Process.Technol. 27, 67-81.

Teng, H.,. Lin Y.U., Hsu, L.Y., 2000. Production of activated carbons from pyrolysis of waste tires impregnated with potassium hydroxide. J. Air Waste Manage. Assoc. 50, 1940–1946.

Ucar, S., Karagoz, S., Ozkan, A.R., Yanik, J., 2005. Evaluation of two different scrap tires as hydrocarbon source by pyrolysis. Fuel 84, 1884-1892.

Xiao, G., Ni, M.J., Chi, Y., Cen, K.F., 2008. Low-temperature gasification of waste tire in a fluidized bed. Energy Convers.Manage. 49, 2078–2082.

**Table captions**

**Table 1**
Proximate and ultimate analyses and gross heating values (GCV)of the solids used.

**Table 2**

Main characteristics of the tyre-derived oil (TDO).

**Table 3**
Composition and HHV of the distillation gas (vol.%).

**Table 4**
Characteristic parameters from TG and DTA curves for distillation-char and coals.

**Table 5**

Characteristics of the gas produced by gasification of different fuels (1000 ºC, 25%$_{vol.}$ $H_2O_{(v)}$ and15%$_{vol.}$ $O_2$).

**Figure captions**

**Fig. 1.** Flowsheet of distillation and gasification process

**Fig. 2.** Flow diagram of the fixed-bed gasification experimental device

(1: HPLC water pump; 2: pressure transducer; 3: steam-gases mixer; 4: hot box heating system; 5: six way valve; 6: hot box; 7: deposit of solids; 8: solids feeding system; 9: reactor; 10: furnace; 11: gas outlet (to micro-GC analysis); 12: pressure regulation valve; 13: liquids condenser; 14: liquids outlet).

**Fig. 3.** Distillation data of tyre derived tyre oil and distillation data of automotive diesel an gasoline oils.

**Fig. 4.** X-ray diffraction patterns of the char obtained in distillation of GST at 550ºC
(Z= Zincite (ZnO), W= Willenite ($Zn_2SiO_4$), and C= carbon

Inset: SEM image which illustrates hexagonal crystalline zincite in the distillation char

**Fig. 5.** SEM image of porosity of the distillation char (DC).

**Fig. 6.** TG (a) and DTA (b) curves for the different coals and distillation char.

**Fig. 7.** DTA curves for combustion of distillation char (DC) at different heating rates.

**Fig.8.** a) Activation Energy (*E*) and pre-exponential factor (*A*) as a function of the reaction progress for the combustion of the distillation char and b) Friedman analysis for the combustion of the distillation char (b)

**Fig. 9**. Main gases production during the gasification of different rank coals and DC at a) 0.1 MPa and b) 1.5 MPa (1000 ºC, 15% $_{vol}$ $O_2$ and 25% $_{vol}$ $H_2$

***Highlights**

The present work had been carrying out from a research collaboration with an industrial partner, which is ending with the building-up in Spain of a pre-industrial plant for the treatment of granulated end-of -life tyres (ELTs), this joint venture also holds the financial support of the Spanish Government.

This work presented the results obtained from the distillation of ELTs and the gasification of the char product obtained from the distillation process.

The results presented here represented a new conception in the treatment of ELTs:

i) As a raw material, its use a granulated ELTs, this is a new material which is being obtaining in installations from Spain and other European countries within the current management systems under use,

ii) The process does not use nitrogen atmosphere (which is typical of classical pyrolisis procedures), thus allowing to obtain a lesser volume of gaseous streams, that, on the other hand, are more rich in organic compounds and thus with a greater GCV, this end in a more adequate electrical co-generation from the gas stream,

iii) The distillation char can be gasified, obtaining a gas product with considerable heating value, especially when gasification proceeds at higher pressure. But also, this char could be co-gasified at existing coal gasification plants without any modification of the gasifier.

iv) Distillation and gasification presents new perspectives for upgrading granulated scrap tyres.

This investigation had been awarded in the 13th Innovation Gallery of the Energy and Environment International Trade Fair (GENERA 2010), held in Madrid (Spain) in May 2010.

Figure

Click here to download high resolution image

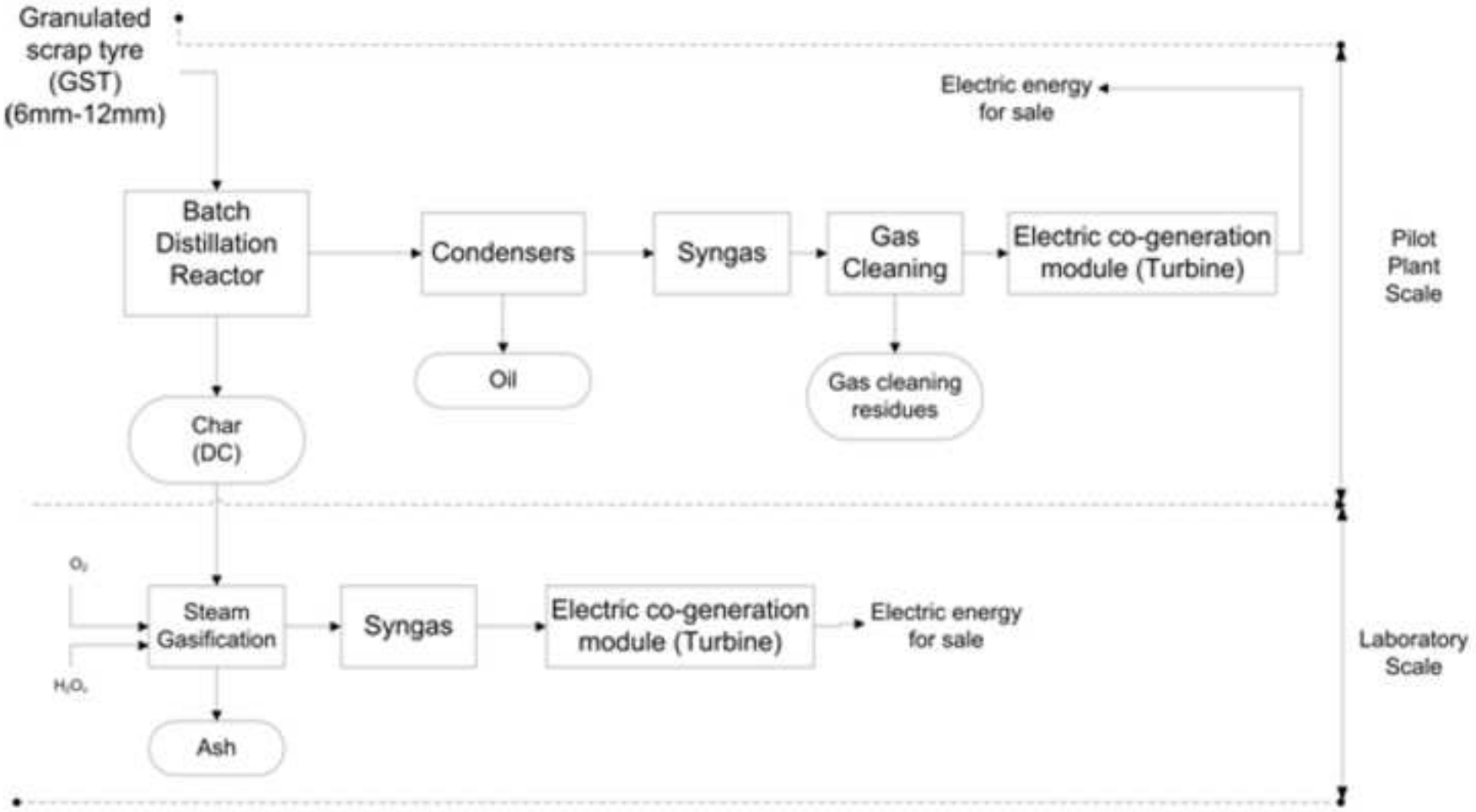

**Figure**

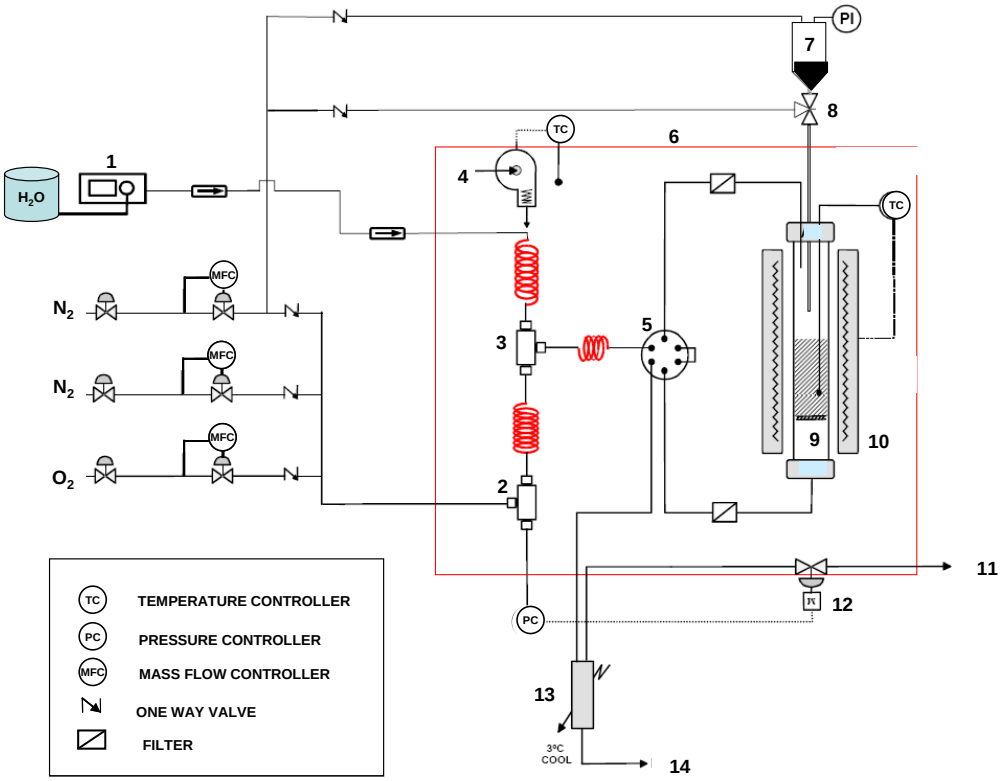


Figure 2

Figure

Click here to download high resolution image

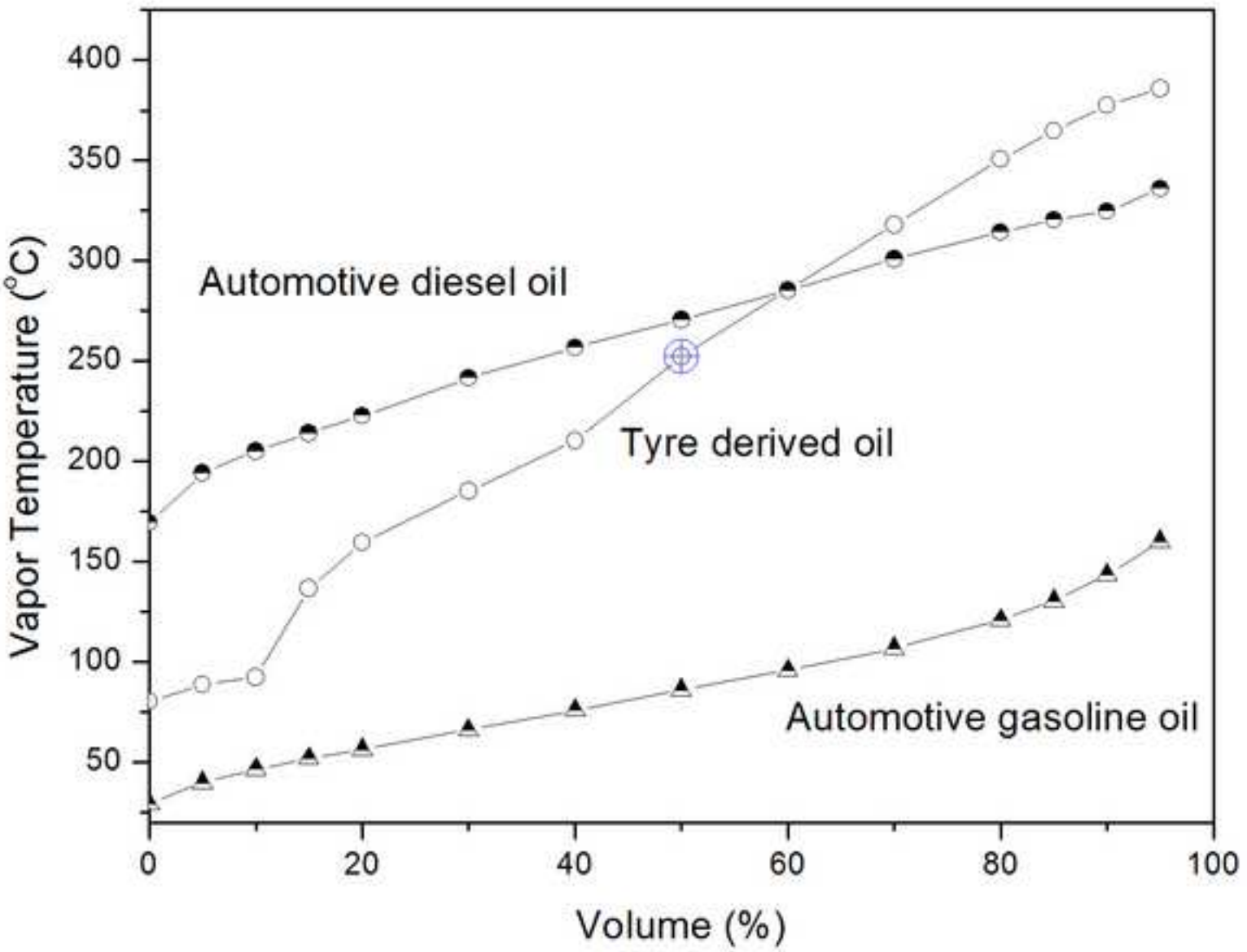

Figure
Click here to download high resolution image

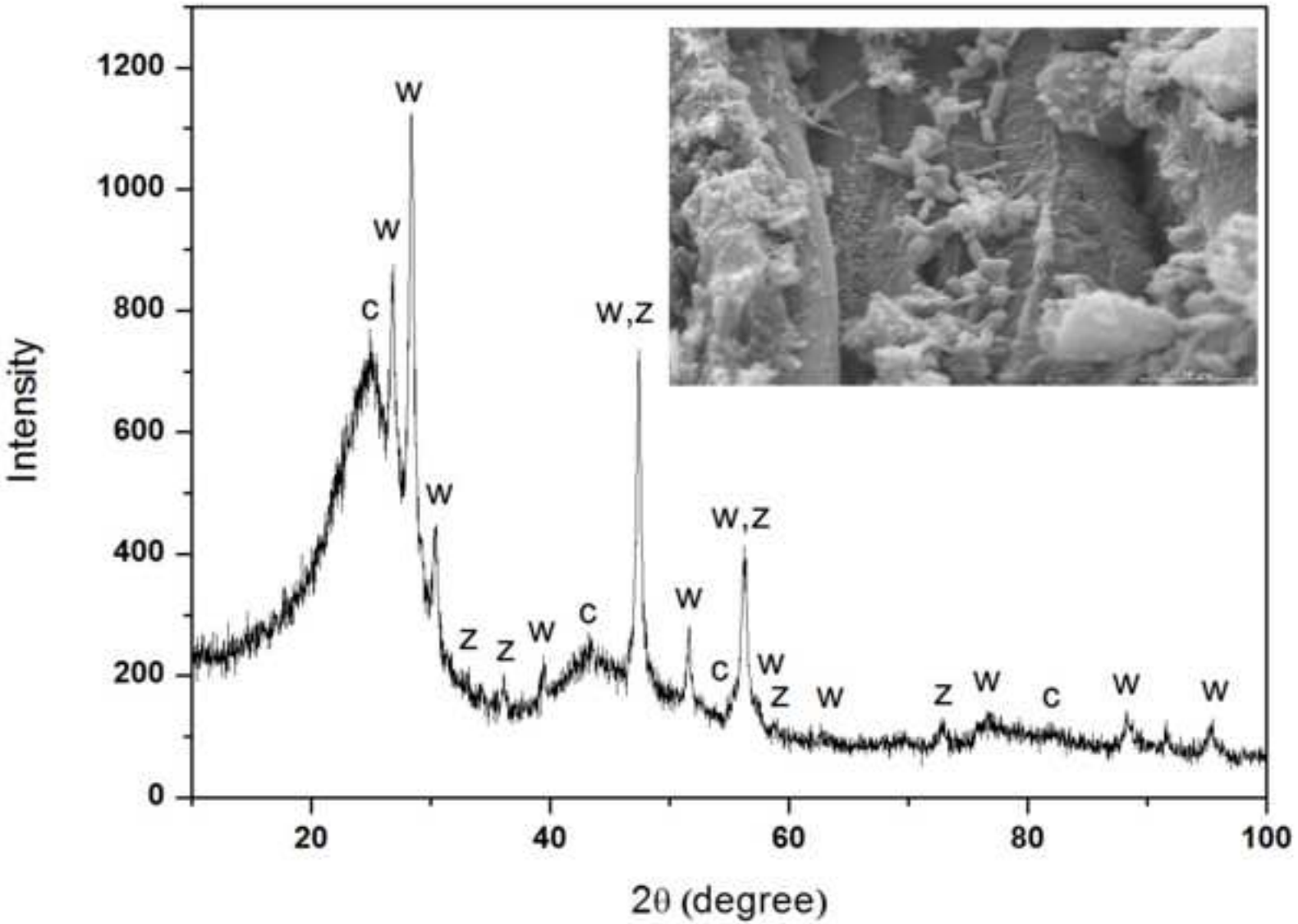

**Figure**

**Click here to download high resolution image**

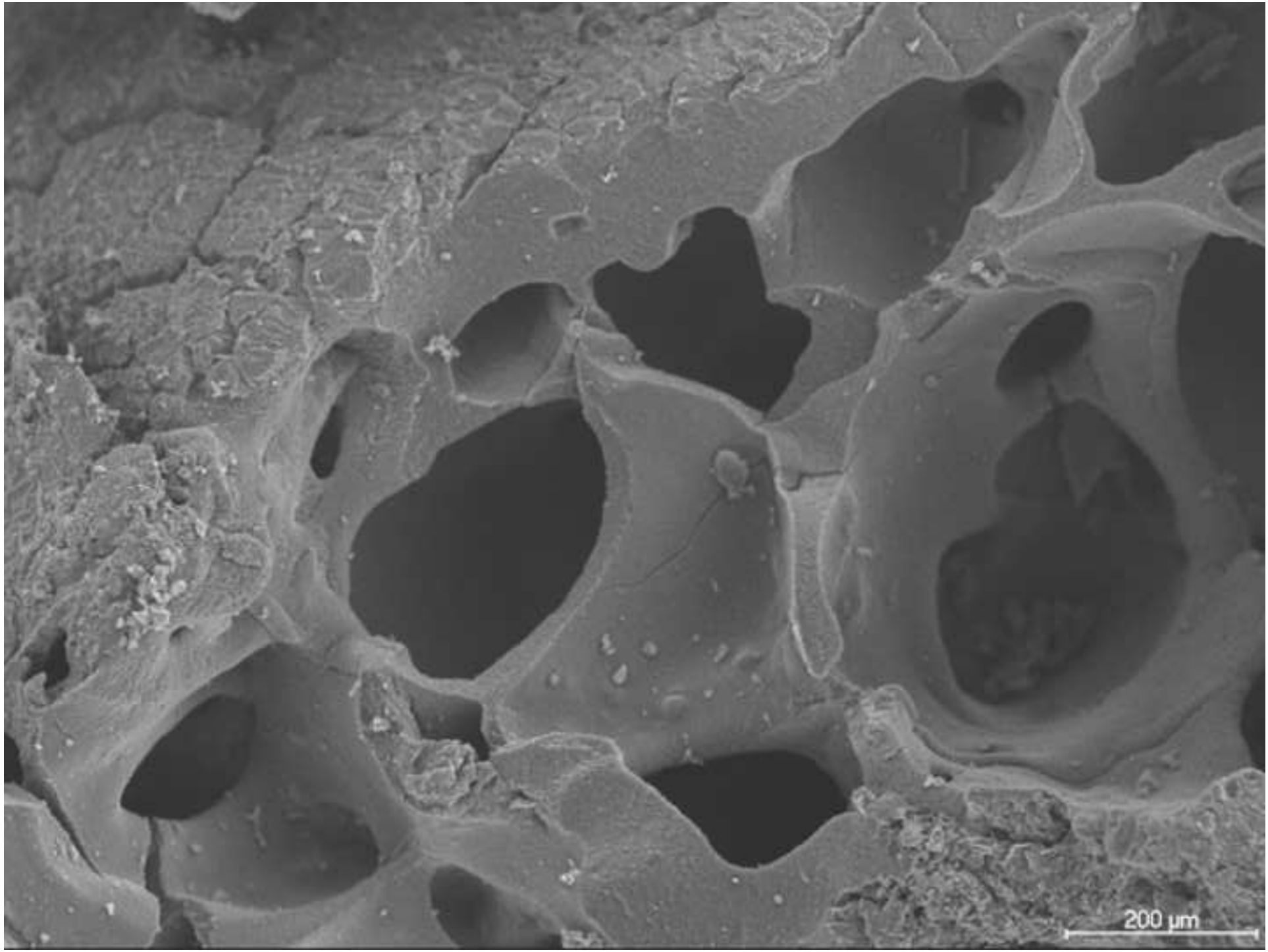

Figure
Click here to download high resolution image

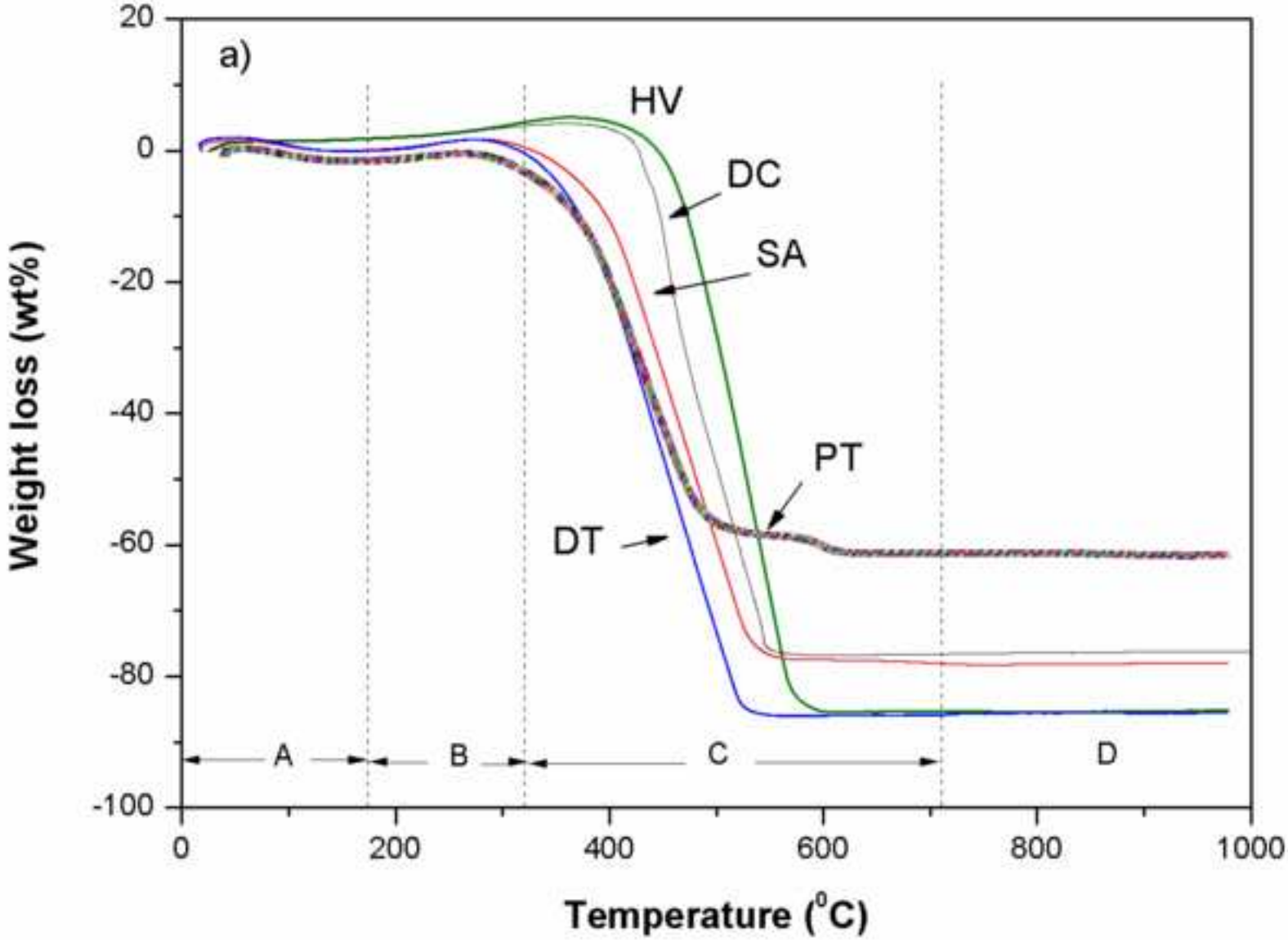

Figure

Click here to download high resolution image

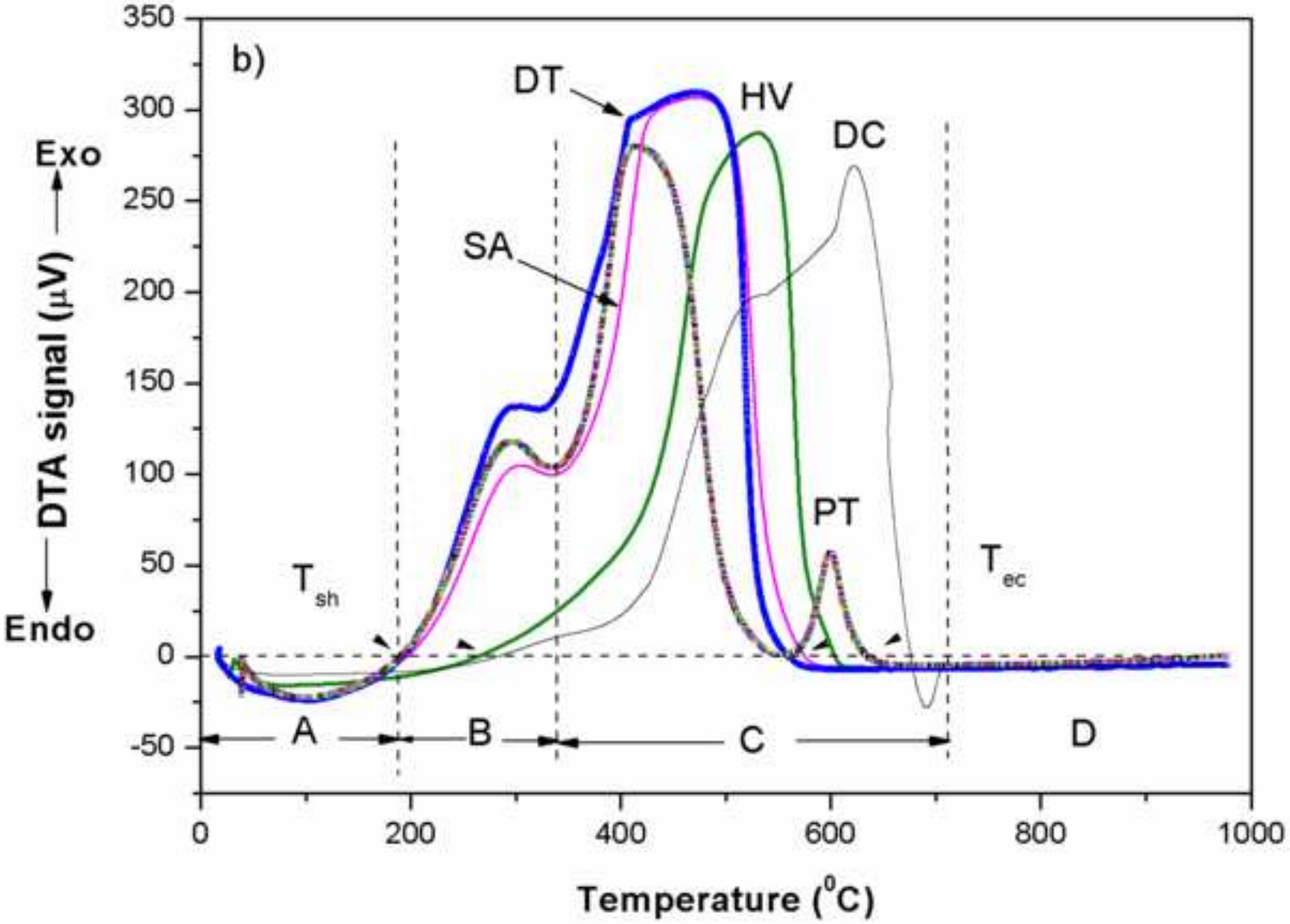

**Figure**

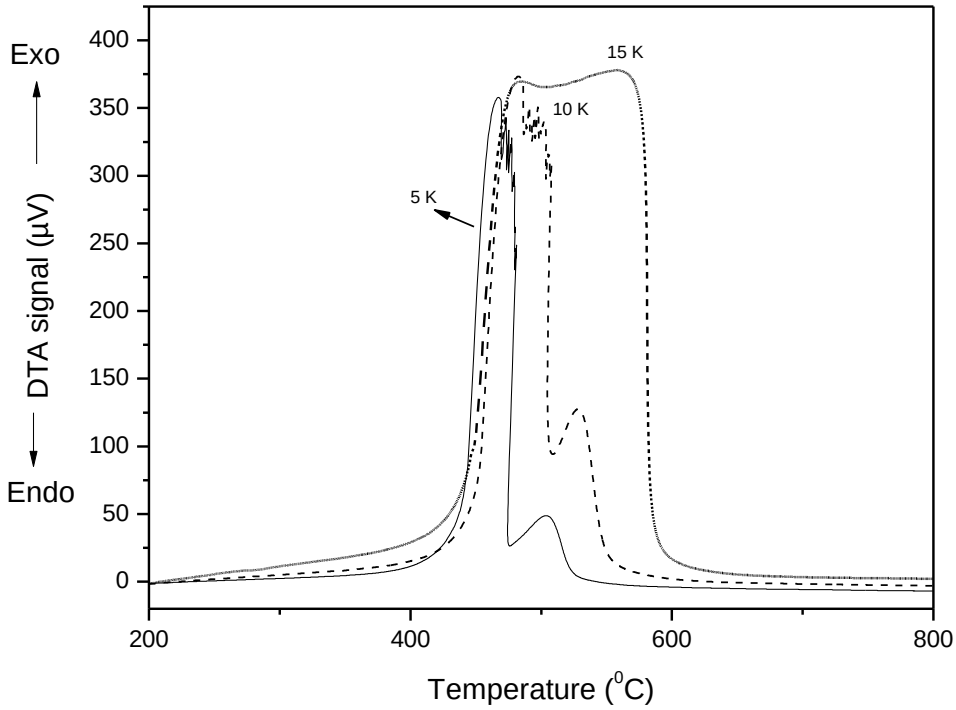
Exo
Endo
DTA signal (µV)
400
350
300
250
200
150
100
50
0
200
400
600
800
Temperature ($^0$C)
15 K
10 K
5 K

Figure

Click here to download high resolution image

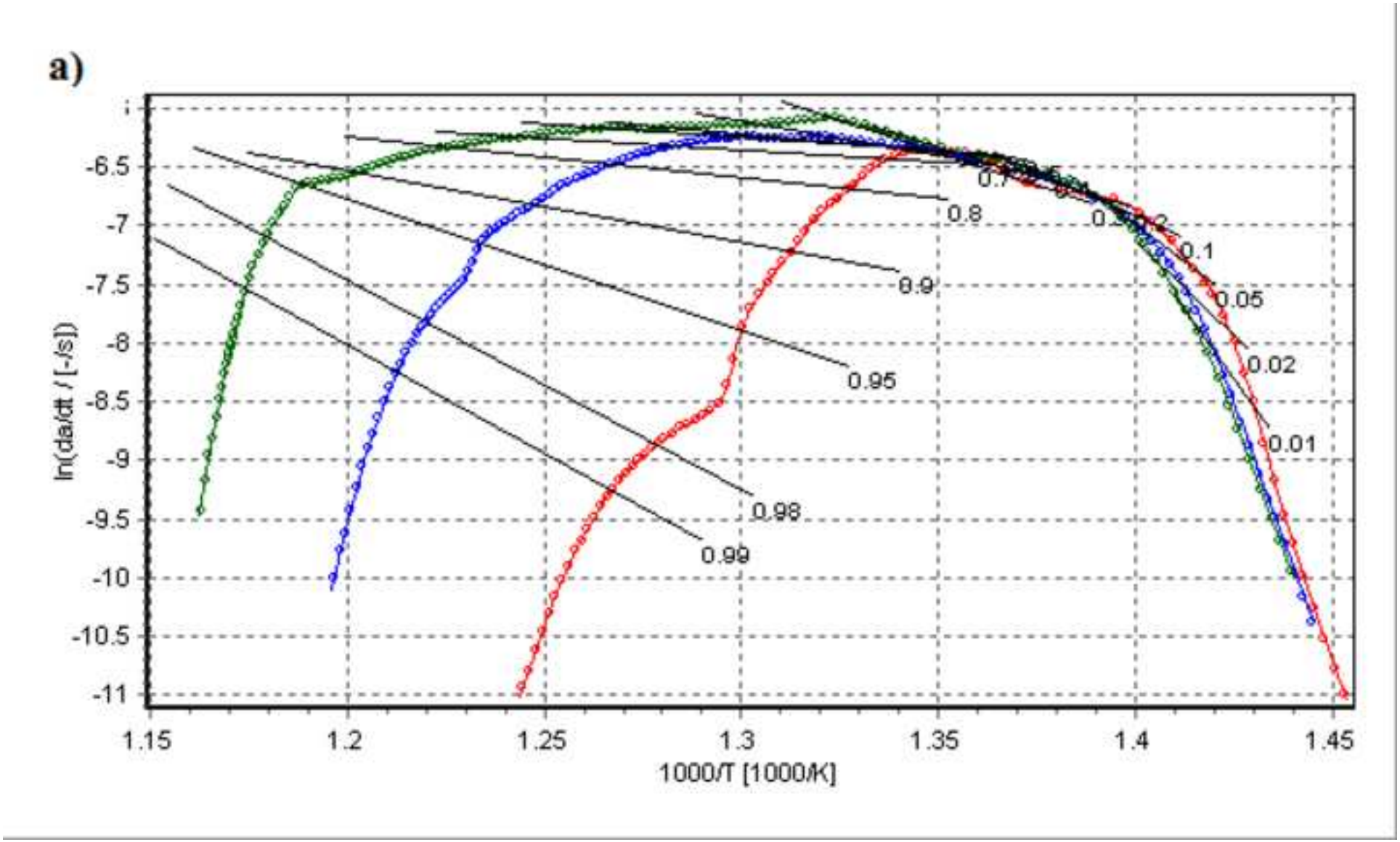

Figure

Click here to download high resolution image

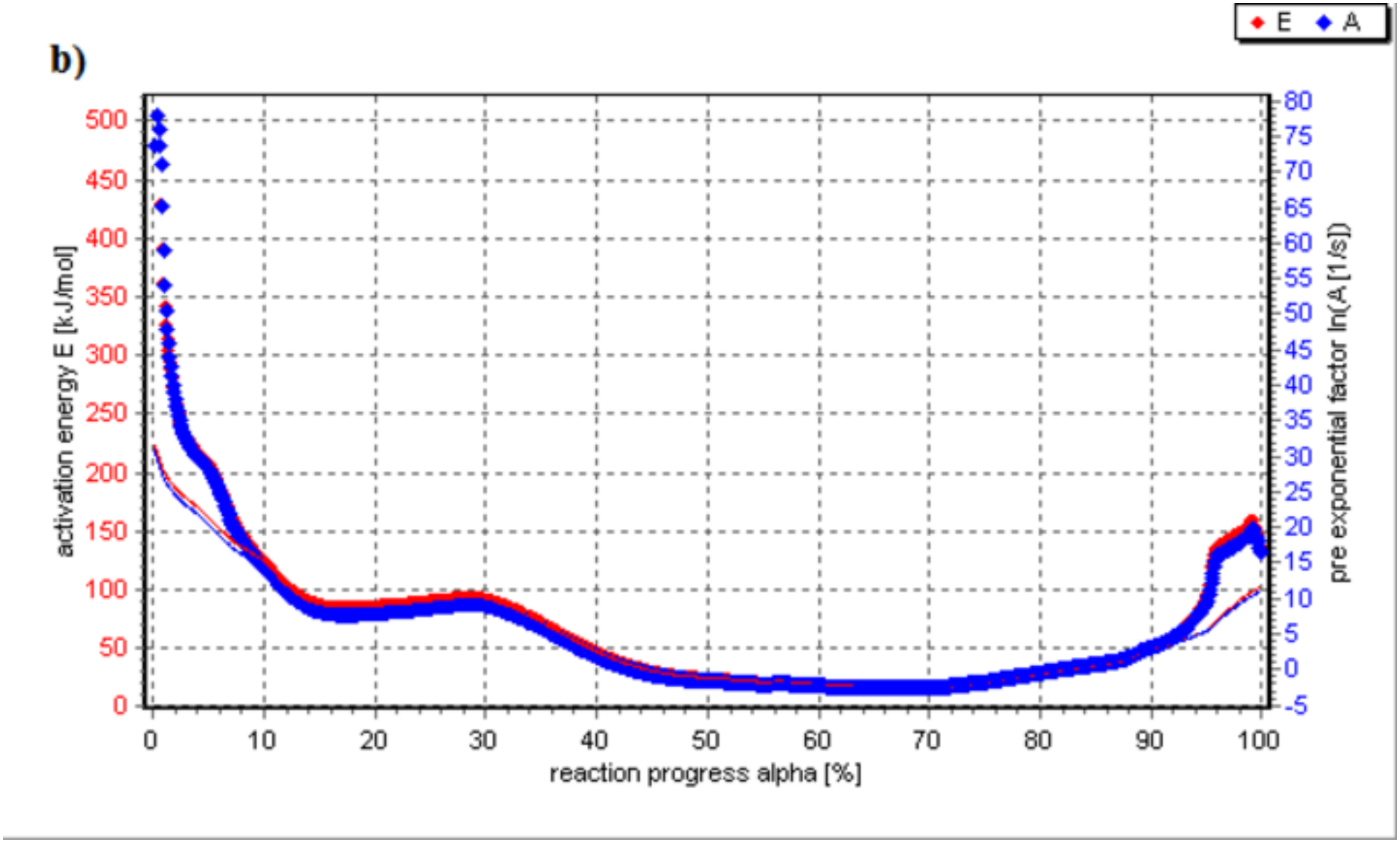

Figure
Click here to download high resolution image

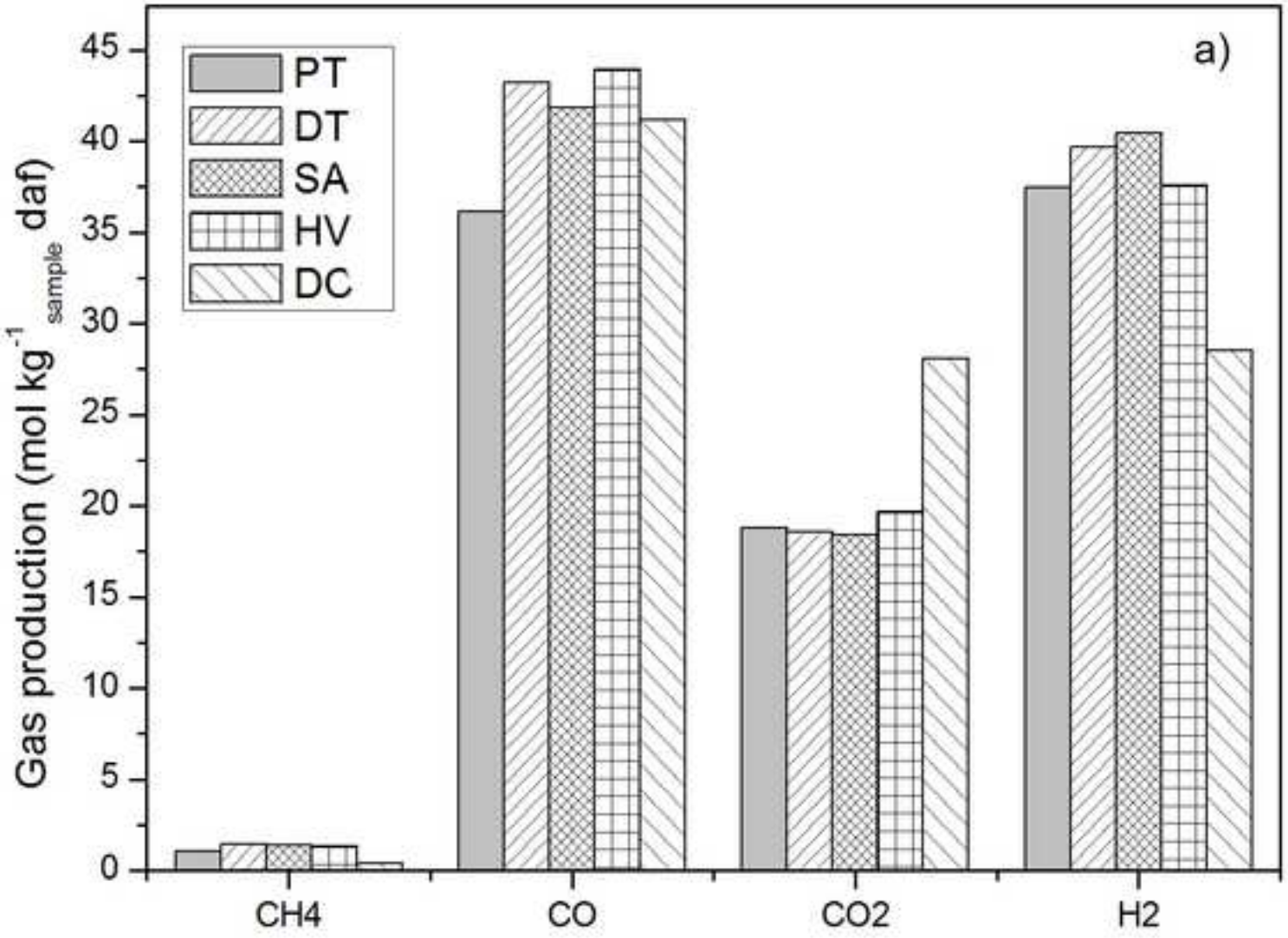

Figure

Click here to download high resolution image

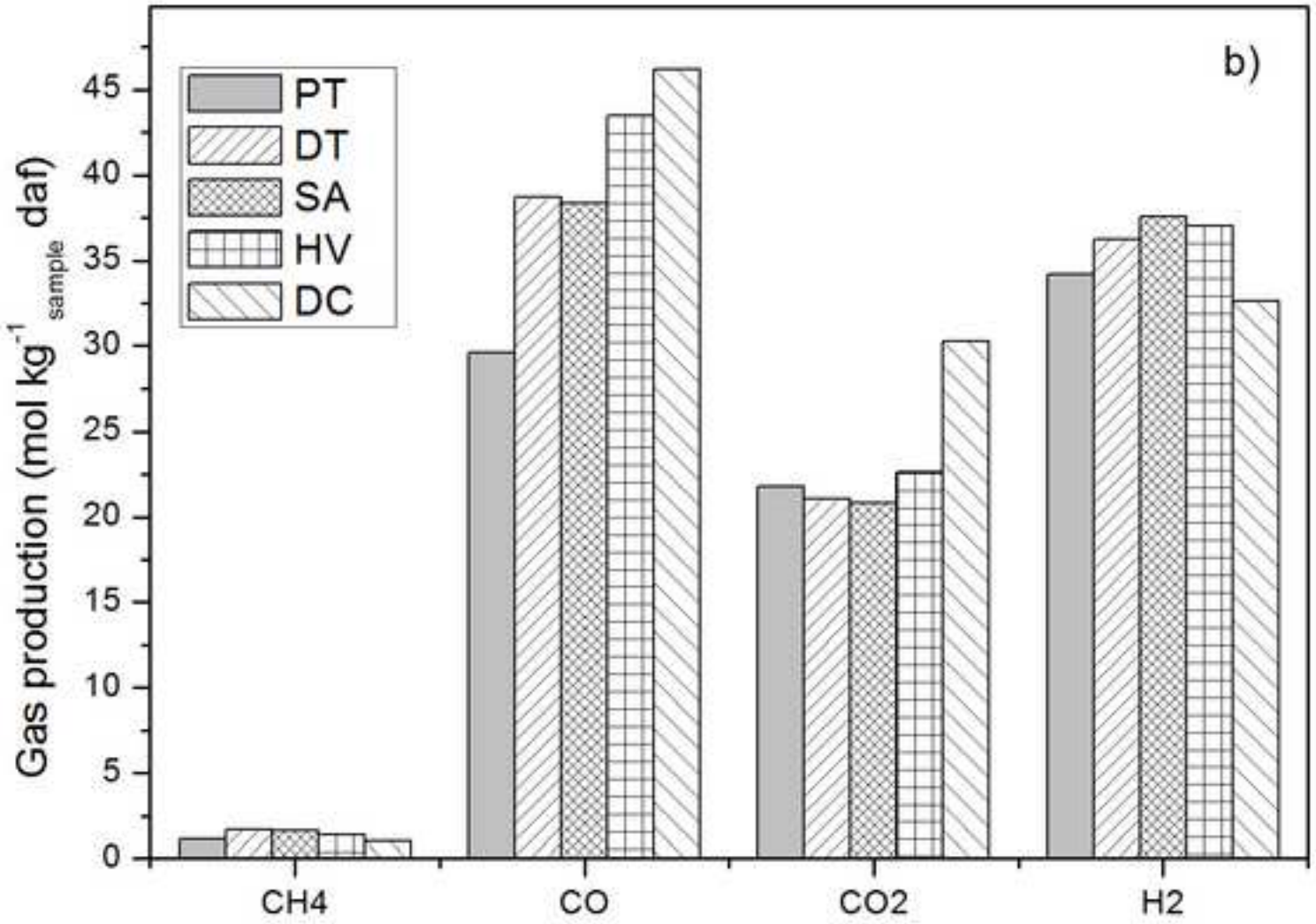

**Table 1**
Proximate and ultimate analyses and gross heating values (GCV)of the solids used.

| Material | Proximate analysis (%wt, db) | | | Ultimate analysis (%wt, db) | | | | | GCV (MJ $kg^{-1}$) |
|---|---|---|---|---|---|---|---|---|---|
| | Volatile matter | Ash | Fixed Carbon | C | H | N | S | O[a] | |
| Granulated scrap tyres (GST) | 66.0 | 4.9 | 29.1 | 86.0 | 8.4 | 0.5 | 1.9 | 3.2 | 38.3 |
| Distillation char (DC) | 1.8 | 12.5 | 85.7 | 86.3 | 0.3 | 0.3 | 2.8 | 10.3 | 29.7 |
| Semianthracite (HV) | 8.6 | 8.8 | 82.6 | 90.6 | 2.8 | 1.7 | 1.9 | 3.0 | 35.1 |
| Medium-volatile bituminous coal (SA) | 25.6 | 14.9 | 59.5 | 78.6 | 4.9 | 1.9 | 0.7 | 13.9 | 32.9 |
| High-volatile bituminous coal (DT) | 29.0 | 10.9 | 60.1 | 81.9 | 5.0 | 0.8 | 1.2 | 11.1 | 32.4 |
| High-volatile bituminous coal (PT) | 24.7 | 36.3 | 39.0 | 71.2 | 4.8 | 1.5 | 1.7 | 20.8 | 29.1 |

[a] Calculated by difference

**Table 2**

Main characteristics of the tyre-derived oil (TDO).

| | |
|---|---|
| C (wt%) | 85.45±0.13 |
| H (wt%) | 11.38±0.25 |
| N (wt%) | 0.44±0.20 |
| S (wt%) | 0.58±0.01 |
| O (wt%, by differ.) | 2.15 |
| H/C atomic ratio | 1.60 |
| GCV (MJ $kg^{-1}$)* | 43.27±0.03 |
| Density at 20 ºC, (kg $m^{-3}$)* | 0.90±0.01 |
| Viscosity at 40º C, (cSt)* | 2.81±0.17 |
| Flash point, (ºC) | 20 |

* Mean value ± standard deviation of at least five distillation runs

**Table 3**

Composition and HHV of the distillation gas (vol.%).

| Gas | Vol. % |
|---|---|
| $H_2$ | 22.27 |
| $O_2$ | 0.73 |
| $N_2$ | 1.86 |
| CO | 1.98 |
| $CO_2$ | 2.54 |
| $CH_4$ | 21.32 |
| $C_2H_4$ (ethene) | 2.32 |
| $C_2H_6$ (ethane) | 4.19 |
| $C_3H_6$ (propene) | 2.80 |
| $C_3H_8$ (propane) | 2.63 |
| $C_4H_8$ (2-butene) | 0.44 |
| $nC_4H_{10}$ (n-butane) | 33.60 |
| $isoC_4H_{10}$ (i-butane) | 1.35 |
| $H_2S$ | n.d. |
| $NH_3$ | n.d. |
| HHV (MJ $kg^{-1}$) | 46.5 |
| HHV (MJ $Nm^{-3}$) | 68.7 |

**Table 4**
Characteristic parameters from TG and DTA curves for distillation-char and coals.

| Sample | $T_{sh}$ (ºC) | $T_{ec}$ (ºC) | Combustion Interval (ºC) | A ($\mu Vsmg^{-1}$) | Ignition | Volatilization and burning | | Char burning | | Burn-out residue† (wt,%) |
|---|---|---|---|---|---|---|---|---|---|---|
| | | | | | Temp. (ºC) | Temp. Range (ºC) | Temp. Peak (ºC) | Temp. Range (ºC) | Temp. Peak (ºC) | |
| DC | 282.4 | 676.0 | 393.6 | $8.8 \cdot 10^3$ | 459 | 283-385 | 330 | 386-688 | 622 | 15.2 |
| HV | 264.1 | 603.8 | 339.7 | $1.17 \cdot 10^4$ | 460 | 287-371 | 350 | 371-695 | 553 | 9.6 |
| SA | 195.3 | 575.4 | 380.1 | $1.05 \cdot 10^4$ | 375 | 195-338 | 303 | 339-591 | 489 | 15.3 |
| DT | 192.9 | 560.1 | 367.2 | $1.13 \cdot 10^4$ | 367 | 193-337 | 283 | 337-560 | 491 | 12.8 |
| PT | 191.0 | 553.6 | 362.6 | $7.8 \cdot 10^3$ | 355 | 191-336 | 285 | 336-554<br>554-655 | 430<br>600 | 38.9 |

($T_{sh}$ = self-heating temperature; $T_{ec}$ = Burn-out temperature; A = Area under DTA curve)

† In the TG curve

**Table 5**

Characteristics of the gas produced by gasification of different fuels (1000 ºC, 25%$_{vol.}$ $H_2O_{(v)}$ and15%$_{vol.}$ $O_2$).

| | Fuel | | | | | | | | | |
|---|---|---|---|---|---|---|---|---|---|---|
| | **PT** | | **DT** | | **SA** | | **HV** | | **DC** | |
| Gas composition (%$_{vol.}$, db) | 0.1 MPa | 1.5 MPa | 0.1 MPa | 1.5 MPa | 0.1 MPa | 1.5 MPa | 0.1 MPa | 1.5 MPa | 0.1 MPa | 1.5 MPa |
| $H_2$ | 19.6 | 18.1 | 18.3 | 17.1 | 19.2 | 18.0 | 16.9 | 15.8 | 11.7 | 12.7 |
| CO | 18.9 | 15.7 | 19.9 | 18.3 | 19.9 | 18.4 | 19.7 | 18.5 | 16.9 | 18.0 |
| $CO_2$ | 9.8 | 11.5 | 8.5 | 9.9 | 8.7 | 10.0 | 8.8 | 9.6 | 11.6 | 11.8 |
| $CH_4$ | 0.5 | 0.6 | 0.7 | 0.8 | 0.6 | 0.8 | 0.6 | 0.6 | 0.2 | 0.4 |
| HHV (kJ $Nm^{-3}$) | 5102 | 4529 | 5114 | 4811 | 5225 | 4929 | 4876 | 4595 | 3702 | 4068 |
| $Y_g$ ($Nm^3$ $kg^{-1}$) | 2.7 | 2.7 | 4.3 | 4.3 | 4.0 | 4.0 | 4.6 | 4.7 | 4.6 | 4.9 |
| $\eta$ (%) | 73.6 | 66.0 | 77.1 | 72.2 | 74.6 | 70.0 | 70.7 | 67.2 | 58.5 | 67.8 |
| X (%) | 92.5 | 88.6 | 93.0 | 92.1 | 93.7 | 92.8 | 87.6 | 87.3 | 87.5 | 97.5 |